Grassi, D., et al. (2017), *Preliminary results on the composition of Jupiter's troposphere in hot spot regions from the JIRAM/Juno instrument*, *Geophys. Res. Lett.*, 44, 4615– 4624, doi:10.1002/2017GL072841

accettato per la pubblicazione il 21 marzo 2017.

Preliminary results on the composition of Jupiter's troposphere in Hot Spot regions from the JIRAM/Juno instrument

D. Grassi[1], A. Adriani[1], A. Mura[1], B.M. Dinelli[2,1], G. Sindoni[1], D. Turrini[1,3], G. Filacchione[1], A. Migliorini[1], M. L. Moriconi[4,1], F. Tosi[1], R. Noschese[1], A. Cicchetti[1], F. Altieri[1], F. Fabiano[5,2], G. Piccioni[1], S. Stefani[1], S. Atreya[6], J. Lunine[7], G. Orton[8], A. Ingersoll[9], S. Bolton[10], S. Levin[8], J. Connerney[11], A. Olivieri[12], M. Amoroso[12]

[1]INAF-Istituto di Astrofisica e Planetologia Spaziali, Roma, Italy
[2]CNR-Istituto di Scienze dell'Atmosfera e del Clima, Bologna, Italy
[3]Departamento de Fisica, Universidad de Atacama, Copiapò, Chile
[4]CNR-Istituto di Scienze dell'Atmosfera e del Clima, Roma, Italy
[5]Dipartimento di Fisica e Astronomia, Università di Bologna, Italy
[6]University of Michigan, Ann Arbor, Michigan, USA
[7]Cornell University, Ithaca, New York, USA
[8]Jet Propulsion Laboratory, California Institute of Technology, Pasadena, California, USA
[9]California Institute of Technology, Pasadena, California, USA
[10]Southwest Research Institute, San Antonio, Texas, USA
[11]NASA Goddard Space Flight Center, Greenbelt, Maryland, USA
[12]Agenzia Spaziale Italiana, Matera, Italy

Key points

- Hot Spots are confirmed as very dry regions in the atmosphere of Jupiter
- Consistent spatial patterns are found in the distributions of water and phosphine
- Ammonia shows local enhancements in the southern parts of Hot Spots

Abstract

The Jupiter InfraRed Auroral Mapper (JIRAM) instrument on board the Juno spacecraft performed observations of two bright Jupiter Hot Spots around the time of the first Juno pericenter passage on August 26th 2016. The spectra acquired in the 4-5 μm spectral range were analysed to infer the residual opacities of the uppermost cloud deck as well as the mean mixing ratios of water, ammonia and phosphine at the approximate level of few bars. Our results support the current view of Hot Spots as regions of prevailing descended vertical motions in the atmosphere, but extend this view suggesting that upwelling may occur at the southern boundaries of these structures. Comparison against the global values of ammonia measured by Juno Microwave Radiometer (MWR) suggests also that Hot Spots may represent sites of local enrichment for this gas. Common spatial patterns in water and phosphine contents are also identified in the two Hot Spots.

1. Introduction

Most of the information currently available on the composition of Jupiter's troposphere derives from remote-sensing data. Among these datasets, a special role has been played by infrared spectroscopy.

While most of the spectrum between 0.4 and 4 μm is dominated by the strong absorption features of methane, a transparent region exists around 5 μm. This region lies far enough from the peak of the solar emission toward the infrared to be largely dominated by the thermal emission of the atmosphere. It hosts the spectral lines of several minor constituents of Jupiter's atmosphere. Among them, H_2O and NH_3 are the main carriers of oxygen and nitrogen in the Jovian envelope, respectively.

The Jovian emission at 5 μm has been measured in the past at low and mid-latitudes with space and ground-based observations [e.g. Fletcher et al., 2016]. Among the bright areas, the so-called 'Hot Spots' stand out as the most intense features. Hot Spots are associated with the grey 'festoons' observed in the optical domain between the Equatorial Zone and the North Equatorial Belt. While their dynamical properties are an active area of investigation [Arregi et al., 2006, Showman and Dowling, 2000], the Hot Spots are long known to be regions of low cloud opacity [Terrile & Westphal, 1977, Ortiz et al., 1998]. In the bright areas, the thermal photons emitted at an effective level of few bars are marginally absorbed by the clouds (i.e.: optical depth < 1), providing an effective probe of the deeper part of the troposphere. The ultimate source of opacity at 5 μm is molecular hydrogen collision-induced absorption, which, even in absence of other minor components or clouds, reaches an optical thickness of 1 around the 5.5 bars level.

Physical conditions in Hot Spots have been measured in great detail by the Galileo Entry Probe (GEP) during its descent on December 7, 1995: the probe entered at 6.5°N 4.9°W, at the southern rim of a Hot Spot [Orton et al. 1998]. While this dataset remains unique in several aspects - notably, the measurements of noble gases [Niemann et al., 1998] - it is still unclear to what extent the abundance of condensable species is actually representative of the conditions of Hot Spots or Jupiter globally.

Most of Jupiter's disk appears dark at 5 μm, implying a global cover of thick clouds. In fact, globally averaged equilibrium thermodynamics models predict three different cloud layers of ammonia, ammonium hydrosulfide and water, extending over several tens of kilometers in altitude [Atreya et al., 1999]. The brightness temperature study by Drossart et al., [1998] demonstrated that at least in the equatorial region the uppermost cloud of NH_3 ice must have residual transparency, allowing some radiation from the warmer regions below to escape to space. Further analysis [Irwin et al., 2001] found that changes in brightness at 5 μm are correlated not with variability of the higher ammonia cloud, but rather with opacity variations associated with cloud layers between 1 and 2 bar pressure.

Properties of Jupiter's atmosphere from the 5-μm radiance have been the subject of several previous studies [Carlson et al., 1993; Roos-Serote et al., 1999, 2004], and, more recently by Giles et al. [2015, 2016]. Five-micron Hot Spots, in particular, have been investigated in detail by a number of researchers [Irwin et al., 1998, Roos-Serote et al., 1998, and Nixon et al. 2001], who analysed mainly the data from Galileo NIMS (near infrared mapping spectrometer).

In this work, we discuss the first observations of the Jovian Hot Spots at 5 μm performed by the Jupiter InfraRed Auroral Mapper (JIRAM) instrument on board the Juno spacecraft [Adriani et al., 2014], during its first perijove passage ("PJ1") on August 26-27, 2016.

2. Dataset

The JIRAM instrument consists primarily of an infrared spectro-imager covering the 2-5 μm range with an average spectral sampling of 9 nm/band (average spectral resolution of 15 nm). JIRAM spectra are often complemented by context images acquired integrating the incoming radiance over a broad spectral range centered around 4.8 μm (M-filter imager). The field of view of individual pixels (for the spectrometer as well as for the imager) is about 240 μrad. Since the spectrometer is acquiring one slit at each Juno spacecraft rotation (2 rpm), consecutive slits are in general not spatially connected.

During the first perijove passage of August 2016, JIRAM obtained a fairly complete spatial coverage of the planet, albeit in a variety of emission angles. The region of expected occurrence of the Hot Spots was observed several times, and this allowed us to select two Hot Spots for a thorough analysis.

1. Hot Spot #1 was centered at 121.7°E, 8.3°N. Individual JIRAM pixels had a size between 501-504 km at the time of the observation. The solar incidence angle ranged between 60° and 70°, while the emission angle ranged between 23° and 35°.

2. Hot Spot #2 was centered at 134.4°W, 7.6°N. Individual JIRAM pixels had a size between 234-237 km at the time of the observation. The solar incidence angle ranged between 80° and 90°, while emission angles ranged between 14° and 28°.

For each Hot Spot, we selected the JIRAM (spectrometer) pixels within 5000 km of the nominal position center for the analysis of the atmospheric composition.

In this preliminary investigation we limited our analysis to the spectral range between 4 and 5 μm. Despite its scientific interest, the inclusion of the solar-dominated 2-4 μm range would require the treatment of solar scattering, with significant computational burden and considerable uncertainties on the forward modeling errors related to the assumptions of the cloud properties (this is especially true for the upper cloud deck and haze). On the other hand, the 'no solar source' approximation is partly justified by our specific focus on these bright areas (assumed to be relatively depleted in clouds), where Drossart et al., [1998] report that scattered solar contribution in the 4-5 region μm should be between 100 and 800 times smaller than the thermal component.

The information content of JIRAM spectra has been discussed extensively in Grassi et al. [2010]. In this analysis, we adapted a Bayesian retrieval code previously developed for the study of VIRTIS-Venus Express data [Grassi et al., 2014]. Free parameters of the spectral fit were (1) the relative humidity of water vapor, (2) the deep (few bars) mixing ratio of ammonia 3) the mean mixing ratio of phosphine (which contributes to the spectral absorption in this spectral region) and 4) the residual opacity of the 1-bar cloud at 5 μm. Relative retrievals errors on these parameters are estimated to be of the order of 10%, and increase to about 20% for ammonia. Performances of the retrieval code have been estimated on the basis of test runs on large sets of simulated observations and the reported retrievals errors include the effects of forward modelling errors in the radiative transfer. Notably, these errors exceed by at least a factor of 10 the instrumental Noise Equivalent Radiance, as recently estimated in Adriani et al. [2016]. More specifically, it turns out that JIRAM benefits from an exceptional signal to noise ratio exceeding 500 in the Hot Spots observation. Under these conditions, it is convenient to quantify the fit quality (quality parameter) as the average relative difference between the best fit and the observed spectrum in a given spectral range (4.6-5 μm in our case) rather than rely on the usual χ^2 value.

3. Results

Figures 1-2 summarize the results of the retrievals for the two Hot Spots.

We will discuss separately the two areas. For the sake of brevity, the standard radiance unit of 1 μW/(cm^2 sr μm) as measured at 4.996 μm is hereafter referred to as 1 RU. The retrieved quantities of panels d.-g. are shown only when the fit quality parameter is smaller than 5%. The retrieved values of the gas parameters (panels e.-g.) are shown only if the corresponding retrieved cloud opacity at 5μ is less than 2.

3.1.Hot Spot #1

Figure 1 presents the results for Hot Spot #1. Its structure appears elongated along the longitude, with an approximate size of 10^4 km by 5 x 10^3 km. The appearance of the Hot Spot is not uniform: at least three distinct radiance maxima can be identified in the brighter area. While the southern rim of the Hot Spot is relatively sharp (rising from <5 RU to 75 RU in about 1500 km), the decrease of the radiance toward the north is much smoother and the boundary of the Hot Spot is blurred in the average brightness of the North Equatorial Belt. Taking into account the different reference wavelength and spectral resolutions, the maximum signal observed in Hot Spot #1 is compatible with the values reported by Roos-Serote et al.,

[1998] and Nixon et al., [2001] for their brighter study cases from NIMS data. The fit quality parameter is not uniform, being considerably better in the regions of high signal. In the southernmost observations over cloudier areas, it exceeds the threshold value of 5% and hence the corresponding pixels are not shown on the maps.

The brightest of several pixels show opacities lower than 0.1, therefore they are considerably more transparent than the ones documented by the Galileo Entry Probe Net Flux Radiometer on its C channel [Sromovsky et al., 1998] or the NIMS real-time spectra discussed by Irwin et al. [1998].

The water relative humidity is below 10% for the entire region where the gas retrievals were performed. Irwin et al. [1998], Roos-Serote et al., [1998] and Nixon et al., [2001] find that bright areas usually appear drier than the surroundings. However, we find that locations where the relative humidity is lower than 1% (e.g.: 7.5°N, 125°E) do not correspond exactly to the brightest regions, but they seem preferentially located on their east side. It should also be noted that our retrieved relative humidity values usually appear a factor of five to eight higher than those found by Roos-Serote et al. [1998] for similar opacity conditions and similarly higher than the values presented by Nixon et al. [2001]. The large-scale latitudinal trends for water vapor presented by Giles et al. [2015] in their Fig. 13 is also only marginally consistent (1.2 ± 0.5%) with our retrievals in the regions surrounding the brightest part of the Hot Spot.

In most of the northern part of the studied region the retrieved value of the ammonia mixing ratio is approximately 200 ppmv, slowly increasing to ~400 ppmv at the southern boundary of the Hot Spot. The ammonia abundance appears to be largely correlated with latitude rather than with absolute radiance and increases steadily toward the equator. Notably, the Juno Microwave Radiometer (MWR) also observed a sharp increase of ammonia moving southward from typical Hot Spot latitudes [Janssen et al., 2017, Li et al., 2017], though the track of MWR did not overpass any of our observed features during the PJ1 passage. A comparison against the *in situ* measurements by the Galileo Probe mass spectrometer [GPMS, Atreya et al., 1999; Wong et al., 2004] or the values derived from probe's radio attenuation data [RA, Folkner et al., 1998] can be properly performed only taking into account the actual pressure range probed by the JIRAM data. Grassi et al. [2010] presented the partial derivatives of JIRAM radiances with respect to ammonia mixing ratio (Fig. 2c and 3b): these functions turned out to be relatively broad, with substantial contributions between 4 and 6.5 bar. The 5-bar level can be roughly assumed as the barycenter of JIRAM sensitivity. On the other hand, the Galileo Probe experiments measured NH_3 as a function of atmospheric pressure. Those data showed that NH_3 was greatly subsolar well below the expected NH_3 cloud base, but reached more than twice the solar value at 5 bars (~330±130 ppmv at 5 bars, Folkner et al., 1998) and a well-mixed value of 700±100 ppmv by RA and 572±218 ppmv by GPMS only at 8 bars, much deeper than the pressure levels probed by JIRAM. The estimates of JIRAM and GEP at the 5 bar level are therefore consistent within the error bars in the entire Hot-Spot #1,with the best agreement being achieved at the southern rim, in a position corresponding to the entry site of the probe.

The phosphine volume mixing ratio varies between $4x10^{-7}$ and $8x10^{-7}$. Its abundance increases from north moving toward the equator, but with a local minimum (9N, 120E) just north of the brightest region of the Hot Spot. Overall, the phosphine values are consistent with the figures reported by Giles et al., [2015, 2016] for global latitudinal trends inferred from VIMS-Cassini data and ground based observations. The phosphine maps presented by Fletcher et al. [2009] also suggest an increase of the mixing ratio from latitude 10N toward the equator. Note, however, that the spectral range used in that work (8-12 μm) probes pressures below 1 bar, lower (hence higher in altitude) than the peaks of JIRAM weighting functions, limiting therefore the validity of a comparison of absolute values.

In the context of JIRAM's data collected during PJ1, Hot-Spot#1 observations were acquired at a relatively large distance and, in a few cases, the spectrometer swaths overlap, allowing an assessment of the robustness of the retrieval scheme. In general, overlapped pixels show highly correlated retrieved values of the atmospheric parameters (differences are within 10% and consistent with systematic spatial gradients), corroborating our confidence in the overall performance of the code.

3.2 Hot Spot #2

Figure 2 presents the results for Hot Spot #2. The structure appears brighter than Hot Spot #1, consistent with the lower emission angle of this observation (which implies a shorter optical path of the line of sight through the residual cloud layer). The size and overall morphology of the structure appears similar to its previously described counterpart Hot Spot #1. Namely, the transparency of the atmosphere appears to have a complex pattern inside the brighter area, with a few local distinct maxima. Similarly, the southern boundary appears sharp, while the Hot Spot tends to disappear more gradually toward north. The range of the observed opacities remains essentially the same in the two regions.

However, some differences can be seen in the gas abundance maps. The water vapor depletion region is more extended toward the north. On the west side of the studied region (138°W, 7.5°N) a number of sites with relatively high relative humidity (>3%) in the transparent regions are visible. Moreover, Hot Spot #2 does not show relative humidity below 1%. Drier areas (but still above 1% relative humidity) are again located immediately east of the brightest pixels.

The ammonia abundances in Hot Spot #2 are consistent with those in Hot Spot #1, but at the southern border of the observed area a few cases of mixing ratios close to 600 ppmv have been observed. Again, this suggests that the values of ammonia are poorly correlated with the overall brightness and are instead driven by latitudinal trends. The more southerly regions of Hot Spot #2 actually appear richer in ammonia than Hot Spot # 1, with the difference being larger than the estimated retrieval uncertainty of 20%. The intrinsic case-to-case variability of these structures represents an important point to consider when comparing JIRAM and Galileo Probe estimates.

Similarly to what observed in Hot Spot #1, the phosphine content tends to increase toward the south, with a latitudinal minimum just north of the brightest area. The range of absolute values of mixing ratios for this molecule is similar in the two areas.

4. Discussions

The JIRAM observations of the two Hot Spots can be summarised as follows:

- In the Hot Spots observed by JIRAM, ammonia increases toward their center, but this trend is most likely related to a general southward increase of ammonia than to a correlation with the brightness itself (panel f. in Figure 2). The ammonia mixing ratios retrieved from JIRAM data are consistent with the range of values (~200-450 ppmv, including error bars) reported by the Galileo Probe for the levels of JIRAM peak sensitivity centered at approximately 5 bars. Our analysis consistently points toward values lower that 600 ppmv, a value reached only in the southernmost boundaries of Hot Spot #2. While this extreme value is still compatible with the deep ammonia values measured by the GPMS experiment *at pressures greater than 8 bars* in another Hot Spot, it appears much larger than the well-mixed value of 350 ppmv obtained by Juno MWR. While the JIRAM values are generally consistent with those derived near the 5-bar level by MWR [Orton et al. 2017] from co-located measurements, we stress that MWR has not yet sampled a Hot Spot directly. A possible scenario therefore seems to be that Hot Spots are sites of anomalous ammonia enhancement, at least in their southern areas.

- Hot Spots show complex patterns in the distribution for the other two observed gases, PH_3 and H_2O. The water vapor content is lower in the brighter regions (as defined by $\tau < 0.3$) than in the surrounding moderate opacity areas. However, drier pixels do not exactly correspond to the brighter ones. Instead, they consistently appear at the immediate east side of the bright regions (compare panels d. and e. in Fig 2). For phosphine, again the overall impression is that its abundance tends to increase toward the south, but a local, moderate decrease is associated with areas just north of more transparent ones (namely, the latitudinal minimum at 8°N in panel g. of Figure 2)

While preliminary, these results confirm that large parts of the Hot Spots are regions of downward motion, related to general dry conditions of the atmosphere. This scheme is also consistent with smaller amounts of

phosphine - considered to be a tracer of upward motions - toward the Hot Spot centers [Fletcher et al., 2009]. The consistent patterns of water vapor (which shows a minimum eastward of the areas of maximum brightness) and phosphine (which shows a minimum northward of the areas of maximum brightness) will be useful in defining an updated dynamical model for these structures. It shall be noted however that our gas mixing ratio maps also suggest the occurrence of *upward* motions of the atmosphere at the southern rims of the Hot Spots: the rise of phosphine and ammonia toward the equator (before the clouds become too thick for JIRAM to provide meaningful measurements) are particularly significant. While MWR provides a clear hint of the rise of ammonia from very deep atmosphere (down to 200 bars) at equatorial latitudes on global scale [Janssen et al, 2017], both JIRAM and – retrospectively – Galileo Probe data suggest further local enhancements of ammonia related to specific conditions within the Hot Spots.

5. Conclusions

JIRAM spectra acquired for two bright Hot Spots during the first Juno perijove passage have been analyzed in the 5-μm transparency window. Our results imply a major role of large-scale latitudinal variations in the abundances of trace gases, with water vapor and phosphine playing an important role as proxies for local Hot-Spot vertical dynamics. The retrieved content of ammonia is also possibly indicative of vertical motions occurring within the Hot Spots.

The results reported in this paper are the first obtained from JIRAM observations and therefore should be regarded as preliminary. The comparison between the ammonia abundances estimated in this work with those measured by the GEP and the Juno MWR will need to be further explored through the additional spectra from PJ1 that have still to be analyzed. Inclusion of shorter wavelength, solar-dominated spectral ranges in the future analyses will provide insights on the cloud structure and allow for testing the preliminary conclusions on vertical dynamics drawn here.

Acknowledgements

This work was supported by the Italian Space Agency through ASI-INAF contract I/010/10/0 and 2014-050-R.0. JIL and SKA acknowledge support from NASA through the Juno Project. GSO acknowledges support from NASA through funds that were distributed to the Jet Propulsion Laboratory, California Institute of Technology.

The retrieval code is based on the ARS software, developed by Nikolay Ignatiev, Space Research Institute of the Russian Academy of Sciences.

Tiziano Maestri (University of Bologna) is acknowledged for his software tools and extensive discussion.

Development of the retrieval code greatly benefited of discussions with P. Irwin, L. Fletcher, R. Giles, T. Fouchet, P. Drossart, M. Roos-Serote and L. Kedziora-Chudczer.

The JIRAM instrument has been developed by Leonardo at the Officine Galileo - Campi Bisenzio site.

The JIRAM instrument was conceived and brought to reality by our late collaborator and institute Director Dr. Angioletta Coradini (1946-2011).

References

Adriani, A. et al. (2014) *JIRAM, the Jovian Infrared Auroral Mapper* Space Sci Rev, doi:10.1007/s11214-014-0094-y

Adriani, A., et al. (2016) *Juno's Earth flyby: the Jovian infrared Auroral Mapper preliminary results*. Astrophysics and Space Science, 361 (8), article id.272.

Arregi, J., et al. (2006) *Phase dispersion relation of the 5-micron hot spot wave from a long-term study of Jupiter in the visible*, Journal of Geophysical Research (Planets), vol. 111, p.9010-doi:10.1029/2005JE002653

Atreya, S. K., et al. (1999). *Comparison of the atmospheres of Jupiter and Saturn: deep atmospheric composition, cloud structure, vertical mixing, and origin*. Planet. Space Sci., 47, 1243-62. doi:10.1016/S0032-0633(99)00047-1

Carlson, B. E. et al. (1993), *Tropospheric gas composition and cloud structure of the Jovian north equatorial belt*, J. Geophys. Res., 98(E3), 5251–5290, doi:10.1029/92JE02737

Drossart, P., et al. (1998), *The solar reflected component in Jupiter's 5-μm spectra from NIMS/Galileo observations*, J. Geophys. Res., 103(E10), 23043–23049, doi:10.1029/98JE01899

Fletcher, L. N., et al. (2009). *Phosphine on Jupiter and Saturn from Cassini/CIRS.* Icarus, 202, 543–564. doi:10.1016/j.icarus.2009.03.023

Fletcher, L. N. et al. (2016) *Mid-infrared mapping of Jupiter's temperatures, aerosol opacity and chemical distributions with IRTF/TEXES*, Icarus, 278, 128-161, doi:10.1016/j.icarus.2016.06.008.

Folkner, W.M. Et al., (1998). *Ammonia abundance in Jupiter's atmosphere derived from attenuation of the Galileo probe's radio signal.* J. Geophys. Res. 103, 22,847-2,856.doi:10.1029/98JE01635

Giles, R.S., et al. (2015) *Cloud structure and composition of Jupiter's troposphere from 5-m Cassini VIMS spectroscopy*, Icarus, 257, 457-470, doi:10.1016/j.icarus.2015.05.030.

Giles, R.S., et al. (2016) *Latitudinal variability in Jupiter's tropospheric disequilibrium species: GeH4, AsH3 and PH3*, accepted for publication in Icarus, doi:10.1016/j.icarus.2016.10.023

Grassi, D. et al. (2010) *Jupiter's hot spots: Quantitative assessment of the retrieval capabilities of future IR spectro-imagers*, Planetary and Space Science, 58, 1265-1278, doi:10.1016/j.pss.2010.05.003.

Grassi, D. et al. (2014) *The Venus nighttime atmosphere as observed by the VIRTIS-M instrument. Average fields from the complete infrared data set*, J. Geophys. Res. Planets, 119, 837–849, doi:10.1002/2013JE004586.

Irwin, P. G. J., et al. (1998), *Cloud structure and atmospheric composition of Jupiter retrieved from Galileo near-infrared mapping spectrometer real-time spectra*, J. Geophys. Res., 103(E10), 23001–23021, doi:10.1029/98JE00948.

Irwin, P. G. J., et al. (2001), *The Origin of Belt/Zone Contrasts in the Atmosphere of Jupiter and Their Correlation with 5-μm Opacity*, Icarus, 149, 397-415, doi:10.1006/icar.2000.6542.

Janssen, M. A., et al. (2017) *The Deep Structure of Jupiter's Atmosphere as Traced by its Subcloud Ammonia Distribution*, Geophys. Res. Lett. This issue.

Li, C., et al. (2017) *Jupiter's global ammonia distribution from inversion of Juno Microwave Radiometer observations* Geophys. Res. Lett. This issue.

Niemann, H. B., et al. (1998), *The composition of the Jovian atmosphere as determined by the Galileo probe mass spectrometer*, J. Geophys. Res., 103(E10), 22831–22845, doi:10.1029/98JE01050.

Nixon, C.A. et al., (2001) *Atmospheric Composition and Cloud Structure in Jovian 5-μm Hotspots from Analysis of Galileo NIMS Measurements*, Icarus, 150, 48-68, doi:10.1006/icar.2000.6561.

Ortiz, J. L., et al. (1998) *Evolution and persistence of 5-μm hot spots at the Galileo probe entry latitude*, Journal of Geophysical Research, vol. 103, p.23051-23069, doi:10.1029/98JE00696

Orton et al., (1998). *Characteristics of the Galileo Probe entry site from earth-based remote sensing observations*. J. Geophys. Res. **103**, 22791-22814

Orton et al. (2017). *Multiple-wavelength sensing of Jupiter from the Juno mission and contemporaneous Earth-based observations.* Geophys. Res. Lett. This issue.

Roos-Serote, M., et al. (1998), *Analysis of Jupiter north equatorial belt hot spots in the 4–5 μm range from Galileo/near-infrared mapping spectrometer observations: Measurements of cloud opacity, water, and ammonia*, J. Geophys. Res., 103(E10), 23023–23041, doi:10.1029/98JE01049.

Roos-Serote, M., et al., (1999) *Constraints on the Tropospheric Cloud Structure of Jupiter from Spectroscopy in the 5-μm Region: A Comparison between Voyager/IRIS, Galileo/NIMS, and ISO/SWS Spectra*, Icarus, 137, 315-340, doi:10.1006/icar.1998.6043.

Sromovsky, L. A., et al. (1998). *Galileo Probe measurements of thermal and solar radiation fluxes in the Jovian atmosphere*. J. Geophys. Res. 103, 22929-22978 doi:10.1029/98JE01048

Showman, A. P., Dowling, T. E. (2000) *Nonlinear simulations of Jupiter's 5-micron hot spots*. Science 289:1737-1740.doi:10.1126/science.289.5485.1737

Terrile, R. J., Westphal, J. A. (1977) *The vertical cloud structure of Jupiter from 5 micron measurements*, Icarus, vol. 30, p.274-281, doi:10.1016/0019-1035(77)90159-2

Wong, M. H., et al., (2004). *Updated Galileo probe mass spectrometer measurements of carbon, oxygen, nitrogen, and sulfur on Jupiter*, Icarus 171 (2004) 153–170 doi:10.1016/j.icarus.2004.04.010

Figure Captions

Fig. 1. Results for Hot Spot #1.
a: Context image from data of JIRAM imager (M-filter at 5 μm). White boxes show the locations of individual pixels of JIRAM spectrometer considered in the analysis. Note that absolute radiometric calibration of JIRAM imager is still in progress and therefore radiometric values shall be considered preliminary
b: Corresponding radiances measured at 4.996 μm by the JIRAM spectrometer
c: Fit quality, quantified as the average relative difference between observed and best-fit spectrum in the range 4.6-5 μm. Only pixels with a fit quality < 5% were retained for subsequent analysis
d. Retrieved cloud opacity (assumed to reside at the 1-bar level) at 4.996 μm. Note the logarithmic scale. Only pixels with $\tau < 2$ were retained for subsequent analysis
e. Retrieved water vapor relative humidity. Note the logarithmic scale.
f. Retrieved ammonia volume mixing ratio
g. Retrieved phosphine volume mixing ratio

Fig. 2. As figure 1, but for Hot Spot #2.

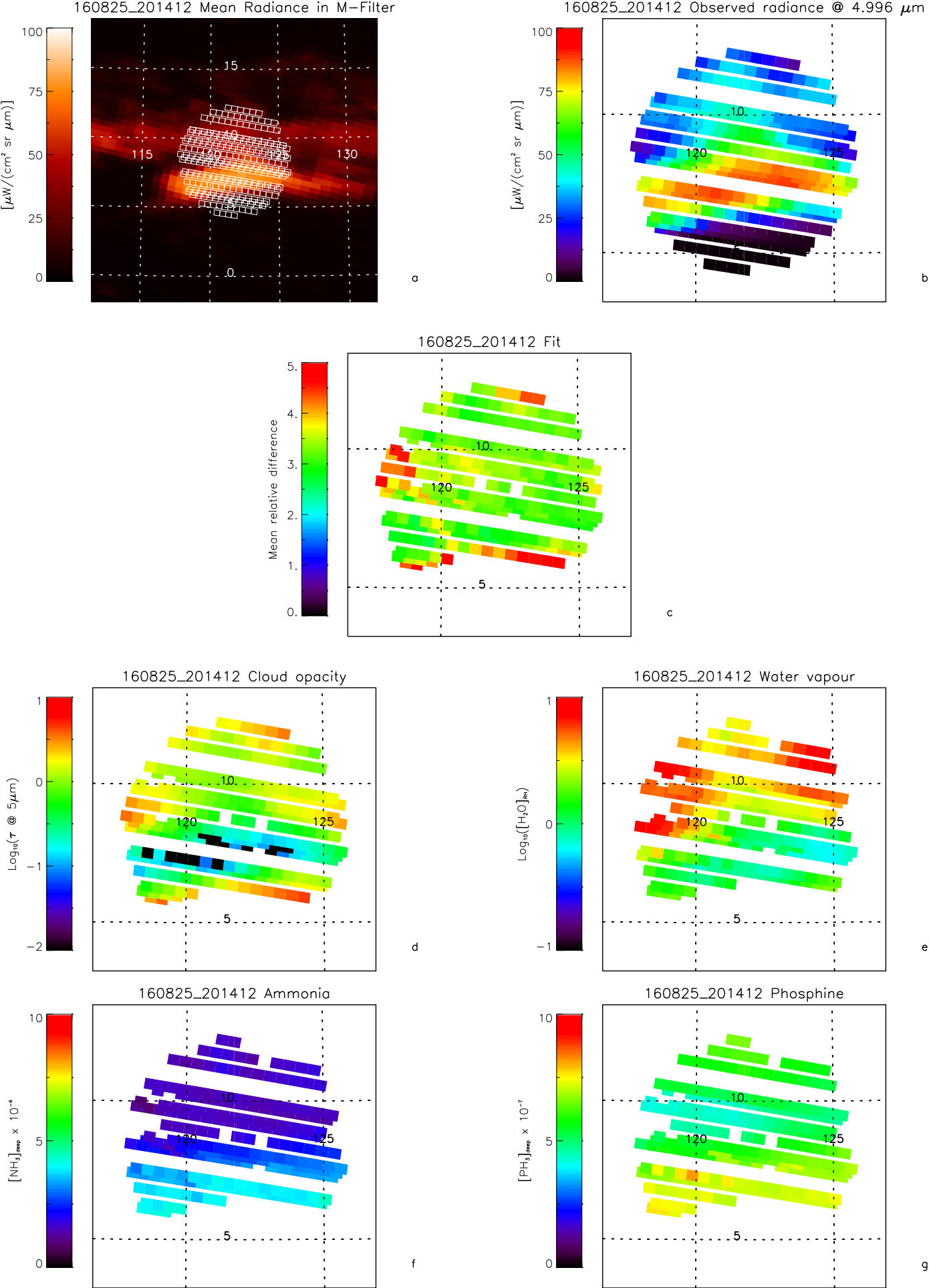
160825_201412 Mean Radiance in M−Filter
[μW/(cm² sr μm)]
100
75
50
25
0
15
10
115
120
125
130
0
a
160825_201412 Observed radiance @ 4.996 μm
[μW/(cm² sr μm)]
100
75
50
25
0
10
120
125
b
160825_201412 Fit
Mean relative difference
5.
4.
3.
2.
1.
0.
10
120
125
5
c
160825_201412 Cloud opacity
Log₁₀(τ @ 5μm)
1
0
−1
−2
10
120
125
5
d
160825_201412 Water vapour
Log₁₀([H₂O]ₛₛ)
1
0
−1
10
120
125
5
e
160825_201412 Ammonia
[NH₃]deep × 10⁻⁴
10
5
0
10
120
125
5
f
160825_201412 Phosphine
[PH₃]deep × 10⁻⁷
10
5
0
10
120
125
5
g

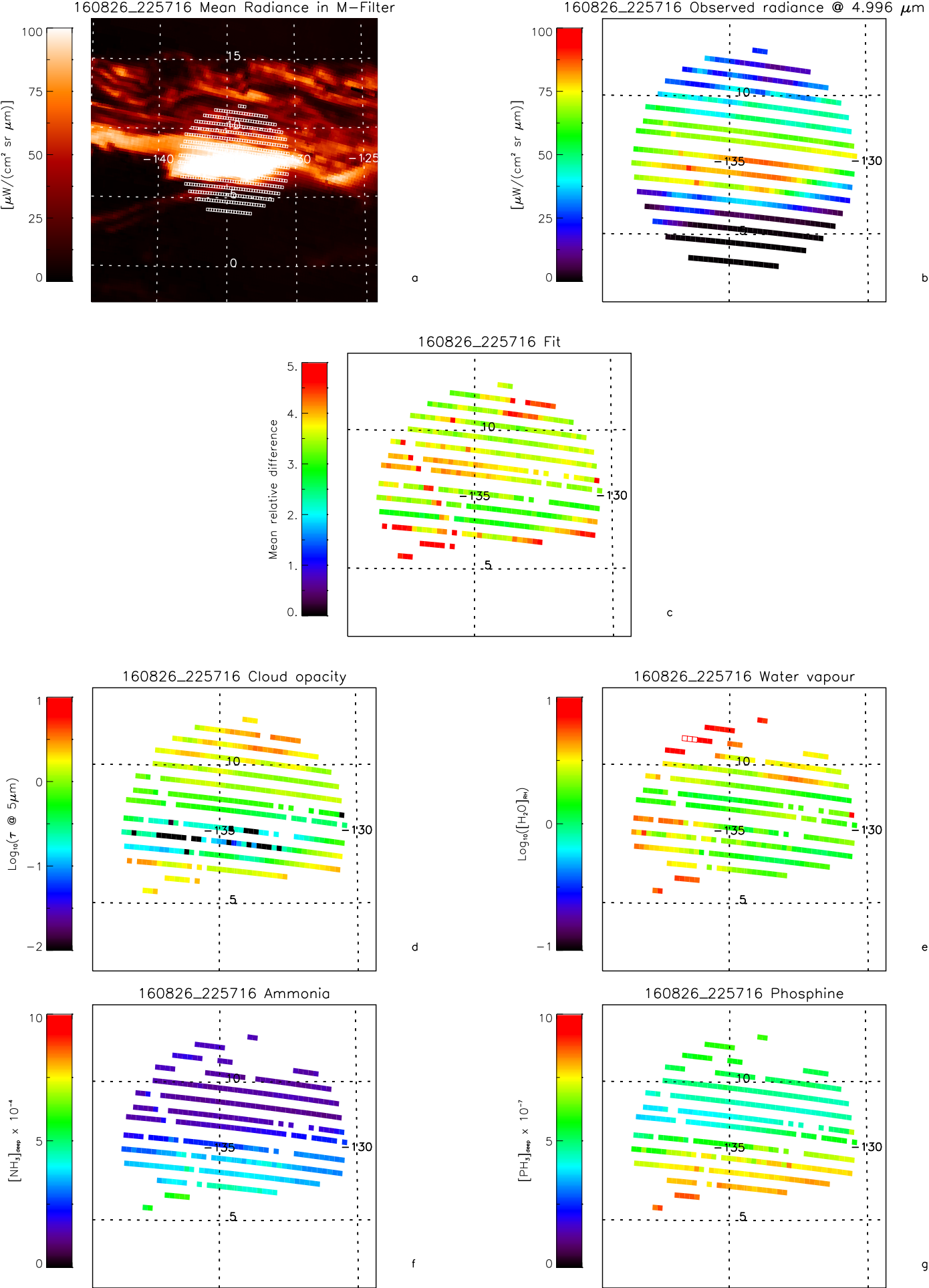
160826_225716 Mean Radiance in M−Filter
[μW/(cm² sr μm)]
100
75
50
25
0
15
10
5
0
−140
30
−125
a
160826_225716 Observed radiance @ 4.996 μm
[μW/(cm² sr μm)]
100
75
50
25
0
10
5
−135
−130
b
160826_225716 Fit
Mean relative difference
5.
4.
3.
2.
1.
0.
10
5
−135
−130
c
160826_225716 Cloud opacity
Log₁₀(τ @ 5μm)
1
0
−1
−2
10
5
−135
−130
d
160826_225716 Water vapour
Log₁₀([H₂O]ₛₜₑₑₚ)
1
0
−1
10
5
−135
−130
e
160826_225716 Ammonia
[NH₃]ₛₜₑₑₚ × 10⁻⁴
10
5
0
10
5
−135
−130
f
160826_225716 Phosphine
[PH₃]ₛₜₑₑₚ × 10⁻⁷
10
5
0
10
5
−135
−130
g